

# Dual Light and Temperature Responsive Micrometer-Sized Structural Color Actuators

Alberto Belmonte, Yera Ye Ussembayev, Tom Bus, Inge Nys, Kristiaan Neyts, and Albertus P. H. J. Schenning\*

Externally induced color- and shape-changes in micrometer-sized objects are of great interest in novel application fields such as optofluidics and microrobotics. In this work, light and temperature responsive micrometer-sized structural color actuators based on cholesteric liquid-crystalline (CLC) polymer particles are presented. The particles are synthesized by suspension polymerization using a reactive CLC monomer mixture having a light responsive azobenzene dye. The particles exhibit anisotropic spot-like and arc-like reflective colored domains ranging from red to blue. Electron microscopy reveals a multidirectional asymmetric arrangement of the cholesteric layers in the particles and numerical simulations elucidate the anisotropic optical properties. Upon light exposure, the particles show reversible asymmetric shape deformations combined with structural color changes. When the temperature is increased above the liquid crystal-isotropic phase transition temperature of the particles, the deformation is followed by a reduction or disappearance of the reflection. Such dual light and temperature responsive structural color actuators are interesting for a variety of micrometer-sized devices.

## 1. Introduction

Liquid-crystalline elastomers (LCEs) are lightly crosslinked materials that combine the properties of an elastomer (entropy elasticity) and a liquid crystal (self-organization). LCEs are appealing as stimuli responsive materials as they exhibit shape-changes upon exposure to external stimuli, such as temperature, light, or magnetic field.<sup>[1–3]</sup> Large shape-changes occur when the LCE experiences a transition from an ordered liquid-crystalline phase to an isotropic phase. The magnitude and direction of this change mainly depends on the orientation of the liquid crystals and the degree of order.<sup>[4]</sup> Most studies are focused on LCE polymer films exhibiting for instance large shape-changes of more than 100%.<sup>[5–7]</sup>

Recently, micrometer-sized LCE actuators have received attention as they are interesting for novel applications, such as microfluidics<sup>[8]</sup> and dynamic surfaces.<sup>[9]</sup> In particular, colloid micrometer-sized systems are interesting because the alignment of liquid crystals can be tuned, resulting in programmed shape-changes.<sup>[10]</sup> For example, Ohm et al.<sup>[11]</sup> showed LCE nematic particles possessing different internal liquid-crystalline alignments which were able to deform upon heating above the isotropic point toward an elongated ellipsoid shape and recover their initial spherical shape upon cooling. The response in most of the LCEs is commonly triggered by heat, while light as a trigger has been rarely reported.<sup>[12–15]</sup> Light actuation allows for spatial-temporal control and can be easily dosed by remote control. In a recent work, Zentel and co-workers<sup>[16]</sup> reported LCE nematic particles exhibiting controlled light actuation up to 40% shape deformation due to the presence of a photoresponsive azobenzene dye anchored to the LCE polymer network.

Chiral nematic or cholesteric liquid-crystalline (CLC) particles are characterized by the presence of a helical twisting of the nematic director.<sup>[17]</sup> Such helical structure exhibits selective Bragg reflection of incident circularly polarized light with the same handedness and at a specific wavelength which depends on average refractive index of the material and the helical pitch, the distance over which a full rotation of the director is completed.<sup>[18,19]</sup> Helical twisting can be obtained and controlled by adding a specific concentration of a chiral dopant molecule to the nematic liquid crystal mixture. The confinement of CLCs in micrometer-sized particles leads to a wide variety of molecular

Dr. A. Belmonte, T. Bus, Prof. A. P. H. J. Schenning  
Stimuli-Responsive Functional Materials and Devices  
Department of Chemical Engineering  
Eindhoven University of Technology  
P.O. Box 513, 5600 MB Eindhoven, The Netherlands  
E-mail: a.p.h.j.schenning@tue.nl


Dr. A. Belmonte, T. Bus, Prof. A. P. H. J. Schenning  
SCNU-TUE Joint Laboratory of Device Integrated Responsive Materials (DIRM)

South China Normal University  
Guangzhou Higher Education Mega Center  
510006 Guangzhou, China

Y. Y. Ussembayev, Dr. I. Nys, Prof. K. Neyts  
Liquid Crystals and Photonics Group  
Department of Electronics and Information Systems  
Ghent University

Tech Lane Ghent Science Park – Campus A 126, 9052 Ghent, Belgium

Prof. A. P. H. J. Schenning  
Institute for Complex Molecular Systems  
Eindhoven University of Technology  
Den Dolech 2, 5600 MB Eindhoven, The Netherlands

 The ORCID identification number(s) for the author(s) of this article can be found under <https://doi.org/10.1002/sml.201905219>.

© 2019 Eindhoven University of Technology. Published by WILEY-VCH Verlag GmbH & Co. KGaA, Weinheim. This is an open access article under the terms of the Creative Commons Attribution-NonCommercial-NoDerivs License, which permits use and distribution in any medium, provided the original work is properly cited, the use is non-commercial and no modifications or adaptations are made.

DOI: 10.1002/sml.201905219

helical arrangements with particular reflection properties which are interesting in research areas, such as optical trapping<sup>[20,21]</sup> and manipulation,<sup>[22,23]</sup> optical sensors,<sup>[24,25]</sup> and lasing.<sup>[26,27]</sup> CLC particles exhibiting both shape and color changes have not been reported so far which can open the gate to a new generation of color- and shape-changing stimuli responsive micrometer-sized objects.

In this work, we fabricate cholesteric LCE micrometer-sized polymer particles exhibiting reversible shape and optical changes<sup>[28,29]</sup> upon both, light exposure and temperature variations. We selected a CLC mixture containing a low amount of crosslinker and used suspension polymerization for the synthesis of the particles. During emulsification an ionic surfactant was added to the water to impose homeotropic anchoring leading to a global anisotropic alignment of the helical structure. After UV-crosslinking, we obtained anisotropic, flexible, and light responsive structural color polymer particles that, upon light exposure and temperature increase, were able to combine asymmetric deformations with red-shifting of the reflection or disappearance of the reflection.

## 2. Results and Discussion

In order to fabricate dual light and temperature responsive micrometer-sized structural color actuators, suspension polymerization of a CLC monomer mixture containing a reactive light responsive crosslinker (1), a nonreactive nematic liquid-crystalline mixture known as E7 (2), a reactive monomer (3), a chiral dopant (4), a photoinitiator (5), and a thermal-inhibitor (6) was used (Figure 1a). The monomer droplets were formed at a temperature above the isotropic point of the CLC mixture ( $T > 54$  °C, Figure S2a, Supporting Information) by emulsification in water containing sodium dodecyl sulfate (7) as surfactant (Figure 1b, step 1). The emulsion was transferred to a thin glass container and cooled down slowly to room temperature to reach the CLC phase (Figure 1b, step 2). During this step, we followed the alignment process by optical microscopy in two monomer droplets having different size (Figure S3, Supporting Information). The droplets undergo a transition from isotropic (black between crossed-polarizers) to the formation of one (small droplet) or multiple (big droplet) off-centered reflective domains suggesting a multimodal configuration of the cholesteric layers.<sup>[30,31]</sup> The CLC polymer particles were formed by UV-exposure through a UV-filter ( $>405$  nm) to prevent azobenzene isomerization (Figure 1b, step 3). Finally, by extracting (2), polymer elastomeric particles were obtained (Figure 1b, step 4) as deduced by the low glass transition temperature ( $T_g \approx 31$  °C) and the presence of an isotropic transition temperature ( $T_{iso}$ ) at  $\approx 114$  °C (Figure S4, Supporting Information). Note that a second transition takes place around  $60$  °C ( $T_{trans}$ ), which might be related to a decrease in the liquid-crystalline order. Scanning electron microscopy (SEM) image (Figure 1c) shows spherical shaped particles of different size with an average diameter of  $7 \pm 5$   $\mu\text{m}$ .

To investigate the optical properties of the particles, we fabricated particles with varying amount of chiral dopant (4) to shift the Bragg reflection band from blue (7 wt%) to infrared (IR) (3.5 wt%) region of the spectrum (Figure 1d; Figure S2b, Supporting Information). In Figure 1e, polarized

optical microscopy (POM) images of the particles reveal spot-like and arc-like reflective colored domains<sup>[32]</sup> ranging from red to green (IR mixture) and green to blue (green mixture). The overall blue-shift of the Bragg reflection of the respective CLC mixtures (Figure S2b, Supporting Information) can be explained by the inherent shrinkage of the helical pitch caused by the extraction of 16.5 wt% of nonreactive monomer (Figure 1b, step 4). However, the presence of multiple colors (i.e., green-to-red in the IR mixture) points to viewing-angle dependency of the Bragg reflection within the particles.

Transmission electron microscopy (TEM) of the cross-section of the particles (Figure 2a) reveal layered patterns that correspond to the cholesteric structures that are differently oriented. Note that the particles exhibit ellipsoidal shapes, which might be due to the deformation of the elastomeric particles during sample preparation. The images have been labeled according to the orientation of the particle. The “top” image reveals nearly parallel stacking of the cholesteric layers which confirms the formation of a bimodal configuration.<sup>[31]</sup> The helical pitch,  $P$ , can be estimated by measuring the distance between three consecutive white stripes, corresponding to  $360^\circ$  rotation of the helical structure, and applied to calculate the reflected wavelength for normal incidence of light,  $\lambda_0$ , according to  $\lambda_0 = P\bar{n}$ , where  $\bar{n}$  is the average refractive index ( $\bar{n} = 1.6$  for common liquid crystals). The calculated  $\lambda_0$  ( $647 \pm 30$  nm, red reflection) is in agreement with the red color that is observed. Both the “side” and “top” images show curvature of the cholesteric layers on one of the edges and planar stacking on the other edge pointing out a deviation with the classical bimodal configuration. The “bottom” image shows different types of cholesteric layer configurations. Here, the folding of the layers (1) is originated mostly at the surface during the relaxation of the cholesteric phase.<sup>[33]</sup> By contrast, the inclination (2) must be formed to solve the connection between the two different edges and the central part of the particle.

We decreased the amount of chiral dopant to 1 wt% (large helical pitch) in order to observe and confirm the alignment of the cholesteric layers by optical microscopy. Typical images taken in transmission and bright-field mode under  $45^\circ$  crossed-polarizers are presented in Figure 2b. The top/side image confirms the formation of two different edges showing a clear transition from planar to curved organization of the layers along the axis. Moreover, both edges (back and front images) exhibit different optical properties which is in agreement with the presence of a single reflective domain observed in the polymer particles with a reflection in the visible wavelength range (Figure 1e). The curvature of the cholesteric layers is attributed to the tendency of the mesogens to align homeotropically to minimize the surface energy during the alignment formation in the presence of sodium dodecyl sulfate as surfactant. However, due to geometrical restrictions of a spherical particle, there are regions in which energetically nonfavored planar stacking occurs.

To identify the origin of the bright reflective colored domains in the CLC polymer particles, we performed numerical simulations on particles with a diameter of  $10$   $\mu\text{m}$ , having planar (helical pitch =  $400$  nm) or curved (in the center helical pitch =  $400$  nm) cholesteric layers (a detailed description of the simulation is provided in the Supporting Information). The reflection for incident monochromatic, red ( $\lambda_0 = 633$  nm) and green ( $\lambda_0 = 532$  nm) beams along the symmetry axis, or

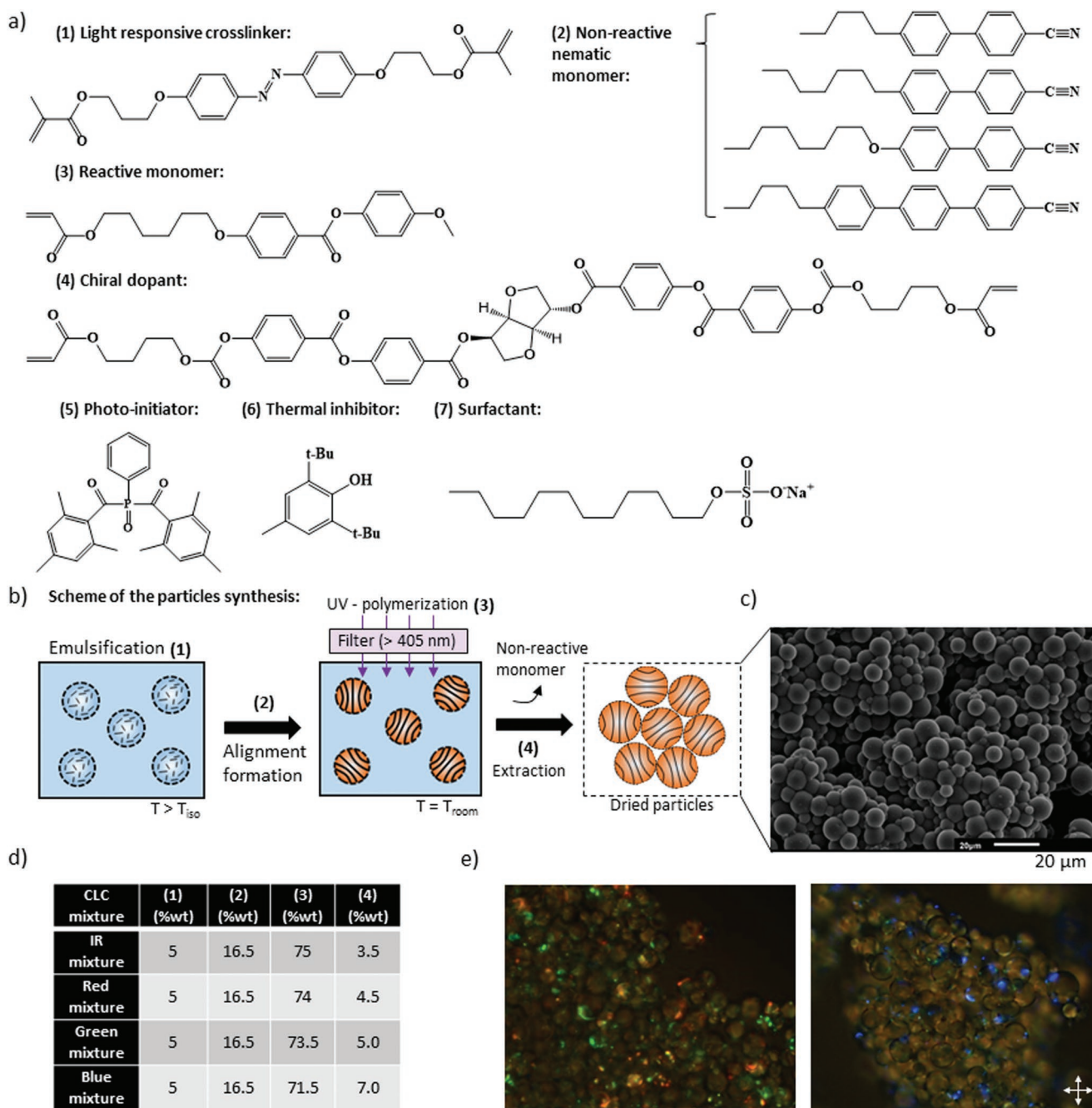


**Figure 1.** a) Chemical structures of cholesteric liquid-crystalline (CLC) monomer mixture, b) scheme of the particles synthesis, c) scanning electron microscopy (SEM) image of the CLC polymer particles, d) composition of CLC monomer mixtures, and e) polarized optical microscopy (POM) images of the CLC polymer particles synthesized with the infrared (IR) mixture (left image) and green mixture (right image).

making an angle of  $30^\circ$  with the symmetry axis was simulated (Figure 3). For light incident along the symmetry axis onto the particle with planar configuration of the layers, a single beam of red light is reflected (left top image) whereas green light is fully transmitted (middle top image). By contrast, for particles with curved layers (right top image) red light is scattered in different directions and the wavelength range is broader. If the planar CLC particle is tilted over an angle of  $30^\circ$  with respect to the incident light, the intensity of the reflected red light drastically

decreases (left bottom image) and a strong green reflection appears (middle bottom image) in accordance with the experimentally observed blue-shift of the Bragg reflection. By contrast, for the particles with curved layers, the intensity of reflected red light is similar to the intensity for  $0^\circ$  incident angle.

Based on the experimental and simulation data, the anisotropic structural and optical properties of the CLC polymer particles can be elucidated. The proposed configuration of the layers depicted in Figure 2c describes the angular-dependent color,



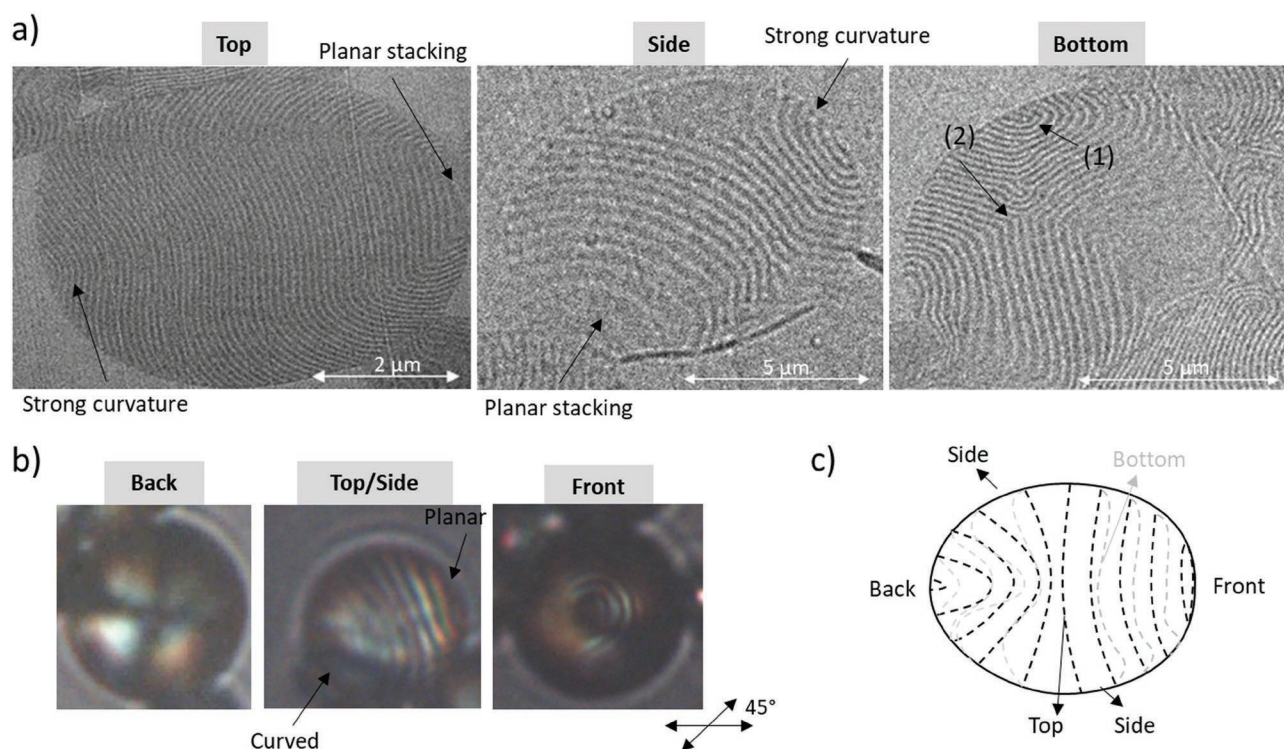


**Figure 2.** Analysis of the cholesteric alignment. a) Transmission electron microscopy (TEM) images of the cross-section of different particles (IR mixture), b) POM images of large-pitch particles, and c) scheme of the cholesteric layers configuration.

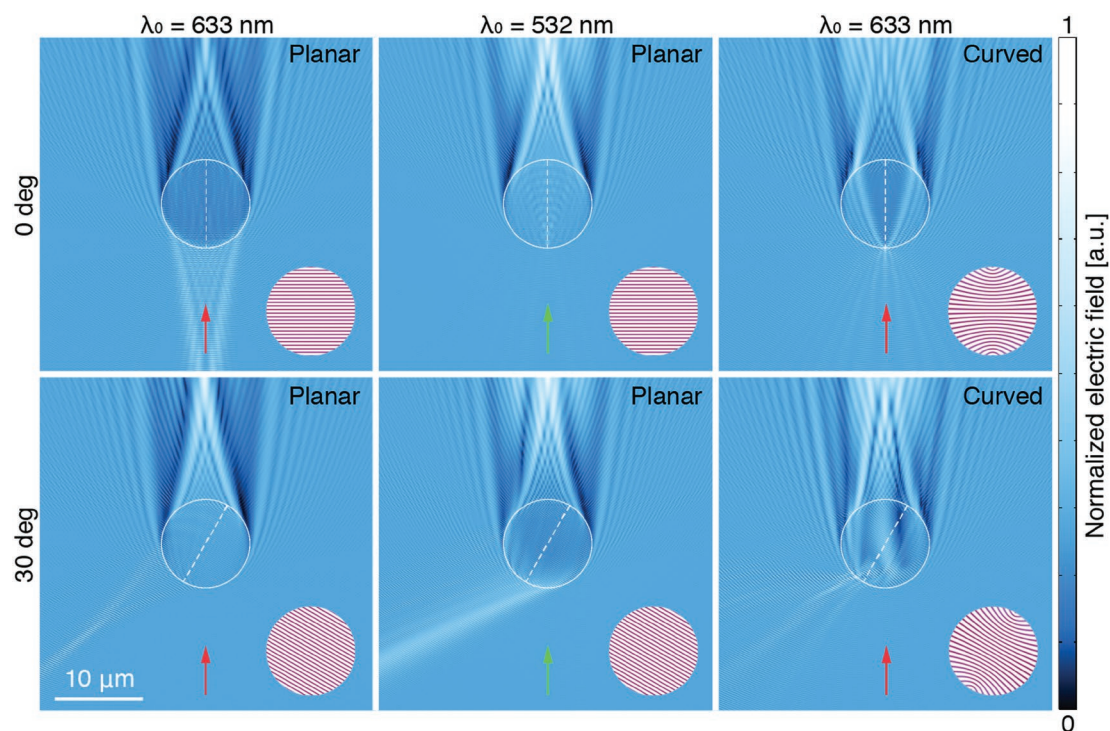


**Figure 3.** Numerical simulations for CLC particles having planar (left and middle columns) or curved (right column) cholesteric layers: particle symmetry axis parallel to the incident light (top row), particle symmetry axis making an angle of  $30^\circ$  with the incident light (bottom row). The red striped circles depict the local director orientation in a section of the particle (the color represents the out of plane component of the director: red when pointing toward the viewer, white when pointing away from the viewer).

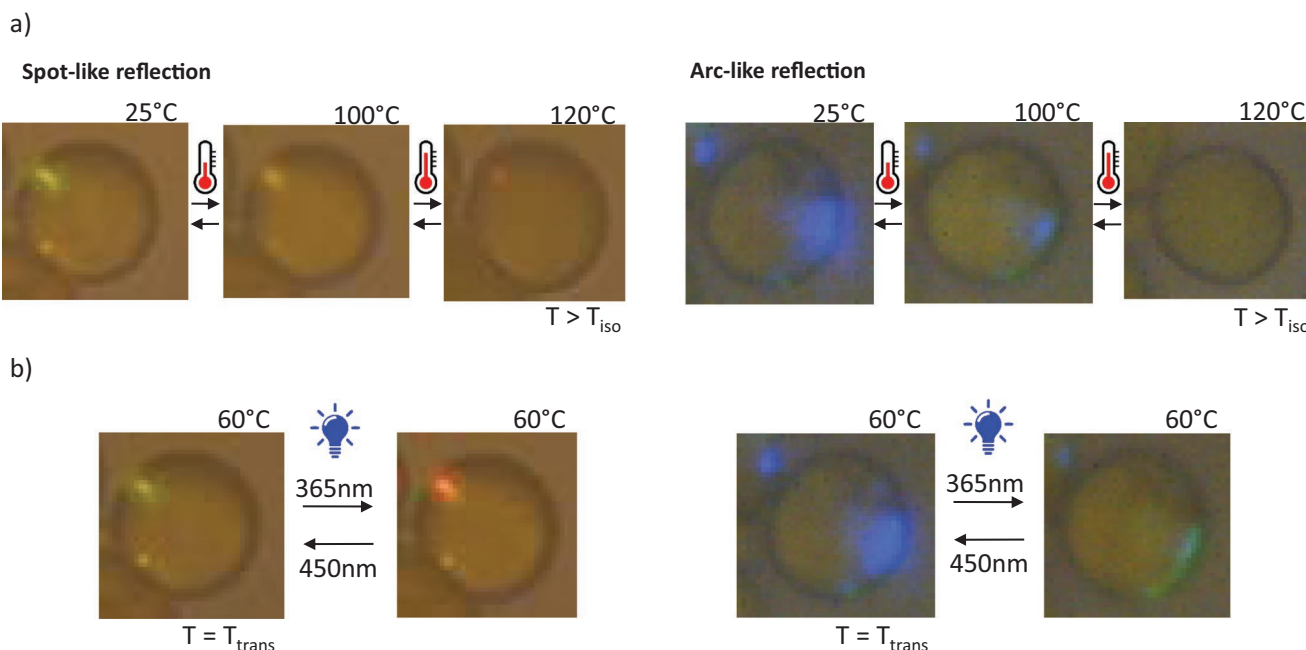


**Figure 4.** a) Temperature and b) light response of particles exhibiting spot-like and arc-like reflective colored domains.

spot-like reflection patterns of the particles. The reflection originates from the planar side, where an angular-dependent bright and narrow-band reflection has been observed in the simulations (Figure 3). For arc-like reflective domains the cholesteric layers at the planar side adopt a deformed arc-like shape as observed in some of the TEM and POM images (Figure 2; Figure S6, Supporting Information). The formation of spot-like, arc-like or multireflective domains is caused by the homeotropic alignment of the mesogens. As proposed by Cipparrone et al.,<sup>[32]</sup> the origin of the helical structure is off-centered in such a case and the exact position of the origin and the size of the particle determine the final configuration of the layers. Spot-like reflective domains are expected for small particles because the origin is situated close to the edge. As the origin approaches the center of the particle, arc-like reflective domains prevail. For large particles, the helical structure grows most likely from more than one nucleus and is therefore difficult to predict.

The temperature and light responsive properties of the CLC polymer particles were studied by optical microscopy (Figure 4; Figure S7, Supporting Information). Particles were dispersed in a refractive index matching oil and first studied by changing the temperature. Upon increasing the temperature (Figure 4a), particles exhibiting spot-like and arc-like reflective domains at room temperature ( $\approx 25\text{ }^{\circ}\text{C}$ ) show a red-shift of the reflected color at  $T = 100\text{ }^{\circ}\text{C} \approx T_{iso}$  and the reflection is significantly reduced or disappears above  $T_{iso}$  ( $T = 120\text{ }^{\circ}\text{C}$ ) (see also Figure S8, Supporting Information). In addition to the color change, the particles show asymmetric deformations (Figure S9a, Supporting Information) and the maximum deformation is observed at  $T > T_{iso}$  ( $120\text{ }^{\circ}\text{C}$ ). When the same particles are exposed to 365 nm UV light during 10 s at a temperature close to  $60\text{ }^{\circ}\text{C}$ , the particles exhibit a red-shift too (Figure 4b; Video S1, Supporting Information). Upon exposure to 450 nm or to normal light, the particles recover to their initial reflection

state. Again, in addition to the red-shift the particles show asymmetric deformations upon light exposure (Figure S9a and Video S2, Supporting Information). It is worth noting that the temperature and light responsive optical and shape changes are fully reversible and can be performed several times.

The asymmetric deformation at  $T > T_{iso}$  is explained by the liquid-crystalline disorder and subsequent shape deformations. Most likely, the reduced order at the molecular level is accommodated by elongation in the helical direction (Figure S9b, Supporting Information). The deformation associated to the UV light exposure at  $T_{trans}$ , by contrast, is related to a photo-mechanical effect. The light responsive moieties absorb UV light inducing stress to the whole network structure due to the trans-cis isomerization. Such stress causes a disorder in the network structure leading to an elongation in the helical direction (see scheme for the light actuation mechanism in Figure S9b, Supporting Information). To verify that the deformation upon UV light is the stress induced rather than the heat, we exposed the particles to 365 nm UV light for 10 s and took POM images after 0, 1, and 5 min (Figure S10, Supporting Information). After 5 min we only observe a minor shape recovery confirming that photothermal effects play a minor role. Elongation of the helical structure also explains the observed red-shift of the reflection color of the particles. In case of light as a stimulus the reflection color remains while in case of a temperature change the color disappears as the temperature is above the isotropic temperature where the cholesteric liquid crystal order is lost.

### 3. Conclusions

Dual light and temperature responsive micrometer-sized structural color actuators based on CLC polymer particles have been synthesized by suspension polymerization. By using a



low amount of a light responsive crosslinker and by imposing homeotropic anchoring conditions, anisotropic, flexible, and light responsive CLC particles have been fabricated. The particles exhibit anisotropic reflective colored domains caused by an asymmetric, nearly parallel configuration of the cholesteric layers with curvature of the layers on one edge and planar arrangement on the other. The particles show reversible deformations and structural color changes upon light exposure and temperature changes. This makes these particles attractive as remotely controlled responsive micrometer-sized devices in application such as optofluidics, optical sensor, and microrobotics.

#### 4. Experimental Section

**CLC Particles Synthesis:** The CLC particles were synthesized by suspension polymerization (Figure S1, Supporting Information). The monomers mixture (Figure 1a) consists of photoresponsive diacrylate (1) (E)-((diazene-1,2-diylbis(4,1-phenylene))bis(oxy))bis(propane-3,1-diyl) bis(2-methylacrylate) purchased from Syncom BV, nonreactive nematic mixture E7 (2) purchased from Merck Chemicals, reactive monoacrylate (3) 4-methoxyphenyl 4-((6-(acryloyloxy)hexyl)oxy) benzoate purchased from Merck Chemicals, and chiral dopant (4) (3R,3aR,6S,6aR)-hexahydrofuro[3,2-b]furan-3,6-diyl bis(4-(((4-(acryloyloxy)butoxy)carbonyl)oxy)benzoyl)oxy)benzoate purchased from BASF. Photoinitiator (5) Irgacure 819 (1% wt) was purchased from CIBA Inc. and thermal-inhibitor (6) (2,6-di-tert-butyl-4-methylphenol, 0.5% wt) was purchased from Sigma-Aldrich. All compounds were used without any further purification. The aqueous phase was formed by dissolving sodium dodecyl sulfate (7) (Sigma-Aldrich) in deionized water ( $30 \times 10^{-3}$  M). The synthesis was carried out in four steps: the formation of the monomer droplets (emulsification), the formation of the cholesteric alignment, the polymerization and the extraction of the nonreactive monomer. For the emulsification, the monomers mixture, photoinitiator, and thermal-inhibitor were first dissolved in dichloromethane and sonicated for 5 min. Then, the solvent was flushed with air and completely evaporated by increasing the temperature up to 80 °C and keeping it for 10 min. Afterward, the preheated aqueous phase (80 °C) was poured onto the melted monomers and the monomer droplets were formed by stirring with an IKA WERKE (Ultra-Turrax T8) at 15 000 rpm for 15 min (Figure S1, step 1, Supporting Information). The emulsion was poured in a preheated glass container with continuous magnetic stirring (300 rpm) and the cholesteric alignment was induced by slowly cooling down to 25 °C (Figure S1, step 2, Supporting Information). Once the temperature was stabilized, the glass container with the emulsion of cholesteric droplets was placed inside a nitrogen box maintaining the stirring at 300 rpm. The polymerization was triggered by exposing the emulsion to UV light at maximum intensity with a mercury lamp (EXFO Omnicure S2000,  $\lambda = 350\text{--}450$  nm) through a >405 nm UV filter for 30 min to ensure full conversion of the acrylate groups (Figure S1, step 3, Supporting Information). Note that the thin glass container helps the UV light to cross throughout the sample and the UV filter prevents the isomerization of the photo-responsive compound. After polymerization, the particles were washed first with ethanol and then twice with tetrahydrofuran to extract the nonreactive monomer (2) (Figure S1, step 4, Supporting Information).

**Characterization Methods:** Thermal transitions of the CLC mixtures and the CLC polymer particles were measured by differential scanning calorimetry using a TA Instruments Q2000 equipment under constant heating-cooling rates of  $10 \text{ }^\circ\text{C min}^{-1}$ . The reflection of the CLC mixtures was measured through UV–vis spectroscopy by using a Perkin Elmer Lambda 750 with a 150 mm integrating sphere over a range of 250–1000 nm (wavelength) at room temperature. Optical images of the CLC mixtures were taken by POM using a microscope (Leica DM2700M) equipped with a Leica MC170 HD high-resolution camera in

reflection mode under crossed-polarizers. The particles size and shape were analyzed by SEM using a JEOL SEM JSM-IT100: the particles were dispersed in sticky conductive film and sputter-coated with a gold target at 60 mA during 30 s.

To follow the cholesteric alignment formation in the monomer droplets under the POM, a drop of the stable emulsion (Figure S1, after step 1, Supporting Information) was poured and spread on a preheated glass plate placed on a heating-cooling Linkam stage. Then, the temperature was slowly cooled down to room temperature ( $5 \text{ }^\circ\text{C min}^{-1}$ ) and images were taken in reflection mode under crossed-polarizers.

The alignment of the cholesteric layers was investigated under TEM of the polymer particles cross-section using a Tecnai 20 (type Sphera) by FEI operating with a LaB<sub>6</sub> filament at 200 kV under slight under-focus conditions. Particles were embedded in an EPOFIX epoxy media. Cross-sections were cut at room temperature using an ultramicrotome (Reichert-Jung Ultracut E) with 60 nm setting thickness. The obtained cross-sections were transferred to a carbon film covered grid (Electron Microscopy Sciences, CF200-CU). The alignment for the large-pitch particles was investigated by POM using a microscope (Leica DM6000M) equipped with a Leica DFC420C high-resolution camera in transmission and reflection mode: the particles were dispersed in a high refractive index-matching oil (poly(methylphenyl)siloxane, PMPS, refractive index  $\approx 1.53$ ) and confined between glass plates leaving 30  $\mu\text{m}$  gap.

To investigate the light and temperature response of the particles, the particles were dispersed in refractive-index matching oil, PMPS, and confined between glass plates as explained above. Then, the cell was placed onto a heating-cooling Linkam stage and the particles were observed by POM at different temperature and light exposure conditions (scheme of the setup is provided in Figure S7).

#### Supporting Information

Supporting Information is available from the Wiley Online Library or from the author.

#### Acknowledgements

This work was financially supported by the Netherlands Organization for Scientific Research (TOP-PUNT 718.016.003).

#### Conflict of Interest

The authors declare no conflict of interest.

#### Keywords

azobenzene, cholesteric liquid crystals, light responsive microactuators, photonic polymer particles, structural colors

Received: September 13, 2019

Revised: October 28, 2019

Published online:

- [1] J. P. F. Lagerwall, G. Scalia, *Curr. Appl. Phys.* **2012**, *12*, 1387.
- [2] R. S. Kularatne, H. Kim, J. M. Boothby, T. H. Ware, *J. Polym. Sci., Part B: Polym. Phys.* **2017**, *55*, 395.
- [3] Y. Yu, T. Ikeda, *Angew. Chem., Int. Ed.* **2006**, *45*, 5416.
- [4] C. Ohm, M. Brehmer, R. Zentel, *Adv. Mater.* **2010**, *22*, 3366.

- [5] A. Belmonte, G. C. Lama, G. Gentile, X. Fernández-Francos, S. De la Flor, P. Cerruti, V. Ambrogio, *J. Phys. Chem. C* **2017**, *121*, 22403.
- [6] M. O. Saed, A. H. Torbati, C. A. Starr, R. Visvanathan, N. A. Clark, C. M. Yakacki, *J. Polym. Sci., Part B: Polym. Phys.* **2017**, *55*, 157.
- [7] G. C. Lama, P. Cerruti, M. Lavorgna, C. Carfagna, V. Ambrogio, G. Gentile, *J. Phys. Chem. C* **2016**, *120*, 24417.
- [8] Y. Hong, A. Buguin, J. M. Taulemesse, K. Kaneko, S. Méry, A. Bergeret, P. Keller, *J. Am. Chem. Soc.* **2009**, *131*, 15000.
- [9] Z. Yang, G. A. Herd, S. M. Clarke, A. R. Tajbakhsh, E. M. Terentjev, W. T. S. Huck, *J. Am. Chem. Soc.* **2006**, *128*, 1074.
- [10] H. Yang, G. Ye, X. Wang, P. Keller, *Soft Matter* **2011**, *7*, 815.
- [11] C. Ohm, C. Serra, R. Zentel, *Adv. Mater.* **2009**, *21*, 4859.
- [12] M. Pilz da Cunha, Y. Foelen, R. J. H. van Raak, J. N. Murphy, T. A. P. Engels, M. G. Debije, A. P. H. J. Schenning, *Adv. Opt. Mater.* **2019**, *7*, 1801643.
- [13] J. A. H. P. Sol, A. R. Peeketi, N. Vyas, A. P. H. J. Schenning, R. K. Annabattula, M. G. Debije, *Chem. Commun.* **2019**, *55*, 1726.
- [14] A. H. Gelebart, D. J. Mulder, M. Varga, A. Konya, G. Vantomme, E. W. Meijer, R. L. B. Selinger, D. J. Broer, *Nature* **2017**, *546*, 632.
- [15] A. H. Gelebart, D. J. Mulder, G. Vantomme, A. P. H. J. Schenning, D. J. Broer, *Angew. Chem., Int. Ed.* **2017**, *56*, 13436.
- [16] L. B. Braun, T. Hessberger, R. Zentel, *J. Mater. Chem. C* **2016**, *4*, 8670.
- [17] Y. Bouligand, F. Livolant, *J. Phys.* **1984**, *45*, 1899.
- [18] M. Moirangthem, A. P. H. J. Schenning, *ACS Appl. Mater. Interfaces* **2018**, *10*, 4168.
- [19] D. J. Mulder, A. P. H. J. Schenning, C. W. M. Bastiaansen, *J. Mater. Chem. C* **2014**, *2*, 6695.
- [20] M. Vennes, S. Martin, T. Gisler, R. Zentel, *Macromolecules* **2006**, *39*, 8326.
- [21] R. J. Hernández, A. Mazzulla, A. Pane, K. Volke-Sepúlveda, G. Cipparrone, *Lab Chip* **2013**, *13*, 459.
- [22] Y. Geng, J. Noh, I. Drevensek-Olenik, R. Rupp, G. Lenzini, J. P. F. Lagerwall, *Sci. Rep.* **2016**, *6*, 2.
- [23] S. J. Aßhoff, S. Sukas, T. Yamaguchi, C. A. Hommersom, S. Le Gac, N. Katsonis, *Sci. Rep.* **2015**, *5*, 14183.
- [24] K. G. Noh, S. Y. Park, *Mater. Horiz.* **2017**, *4*, 633.
- [25] J. H. Jang, S. Y. Park, *Sens. Actuators, B* **2017**, *241*, 636.
- [26] D. E. Lucchetta, F. Simoni, R. J. Hernandez, A. Mazzulla, G. Cipparrone, *Mol. Cryst. Liq. Cryst.* **2017**, *649*, 11.
- [27] M. Humar, I. Mušević, *Opt. Express* **2010**, *18*, 26995.
- [28] Y. Wang, H. Cui, Q. Zhao, X. Du, *Matter* **2019**, *1*, 626.
- [29] F. Fu, L. Shang, Z. Chen, Y. Yu, Y. Zhao, *Sci. Rob.* **2018**, *3*, eaar8580.
- [30] D. Seč, T. Porenta, M. Ravnik, S. Žumer, *Soft Matter* **2012**, *8*, 11982.
- [31] M. N. Krakhalev, A. P. Gardymova, O. O. Prishchepa, V. Y. Rudyak, A. V. Emelyanenko, J. H. Liu, V. Y. Zyryanov, *Sci. Rep.* **2017**, *7*, 14582.
- [32] G. Cipparrone, A. Mazzulla, A. Pane, R. J. Hernandez, R. Bartolino, *Adv. Mater.* **2011**, *23*, 5773.
- [33] D. Seč, S. Čopar, S. Žumer, *Nat. Commun.* **2014**, *5*, 3057.